Essential function of Mec1, the budding yeast ATM/ATR checkpoint-response kinase, in protein homeostasis

Cha, Rita; Corcoles Saez, Isaac; Dong, Kangzhen; Johnson, Anthony; Waskiewicz, Erik; Costanzo, Michael; Boone, Charles

Developmental Cell

DOI:
10.1016/j.devcel.2018.07.011

Published: 20/08/2018

Peer reviewed version

Essential function of Mec1, the budding yeast ATM/ATR checkpoint-response kinase, in protein homeostasis

Isaac Corcoles-Saez[1], Kangzhen Dong[1], Anthony L. Johnson, Erik Waskiewicz, Michael Costanzo[2], Charles Boone[2], and Rita S. Cha[3]

North West Cancer Research Institute, School of Medical Sciences, Bangor University, Deniol Road, Bangor, LL57 2UW, United Kingdom.

[1] These authors contributed equally to this work.

[2] University of Toronto, Donnelly Centre, 160 College Street, Toronto, Ontario, M5S 3E1, Canada.

[3] Correspondence: r.cha@bangor.ac.uk.

ABSTRACT

Unlike most checkpoint proteins, Mec1, an ATM/ATR kinase, is essential. We utilized *mec1-4,* a missense allele (E2130K) which confers diminished kinase activity, to interrogate the question. Unbiased screen for synthetic interactors of *mec1-4* identified numerous genes involved in protein homeostasis. *mec1-4* confers sensitivity to heat, an amino acid analogue, and Htt103Q, a pathogenic model peptide of the Huntington's disease protein. Oppositely, *mec1-4* confers robust resistance to cycloheximide, a translation inhibitor. In response to heat, *mec1-4* leads to widespread protein aggregation and cell death. Activation of autophagy promotes aggregate-resolution and rescues *mec1-4* lethality. Key components of the Mec1 signalling network, $Rad53^{Chk1}$, Dun1, and Sml1, also impact survival in response to proteotoxic stress. These findings show that proteostasis is a fundamental function of Mec1 and that Mec1 is likely to utilize its checkpoint response network to mediate resistance to proteotoxic stress, a role that may be conserved from yeast to mammalian cells.

INTRODUCTION

The ATM/ATR family proteins are conserved serine/threonine kinases best known for their roles in DNA damage- and replication stress- checkpoint response (Harper and Elledge, 2007; Jeggo et al., 2016). They are also involved in a number of fundamental processes including DNA replication, meiotic recombination, and mitochondrial respiration (e.g. Carballo et al., 2008; Cha and Kleckner, 2002; Yi et al., 2017). In humans, inactivation of ATM and ATR leads to Ataxia-Telangiectasia (A-T) and Seckel syndrome, respectively, debilitating diseases characterized by a constellation of symptoms, including neuronal degeneration, cancer, diabetes, microcephaly, and meiotic dysfunction (Shiloh and Kastan,

2001).

Budding yeast genome encodes for two ATM/ATR kinases, Tel1 and Mec1, which share 22.3% and 23.7% identity with the mammalian ATM and ATR, respectively. In comparison, the identity shared between Tel1 and ATR is 19.6% and between Mec1 and ATM is 17.8%. Based on these considerations, Mec1 and Tel1 are generally regarded as the budding yeast ATR and ATM, respectively. However, Mec1 performs most functions of both ATM and ATR, while deletion of *TEL1* does not confer any obvious phenotypes (e.g. Mallory and Petes, 2000).

Mec1 is unusual among checkpoint proteins because it is essential for viability. This requirement can be bypassed by Rnr1 overexpression or deletion of *SML1* (Desany et al., 1998; Zhao et al., 1998). Rnr1 is an essential catalytic subunit of ribonucleotide reductase (RNR), a conserved holoenzyme required for *de novo* dNTP production. Sml1 is an Rnr1 inhibitor and is degraded in response to genotoxic/replication stress via the Mec1-Rad53-Dun1 signalling cascade (Zhao et al., 1998; Chabes et al., 1999; Zhao et al., 2001). Rad53 is an essential downstream kinase of Mec1 and an ortholog of the Chk1 tumour suppressor (Sanchez et al., 1999). Dun1 is a protein kinase that phosphorylates Sml1, facilitating its ubiquitin dependent destruction (Zhao and Rothstein, 2002). Viable *mec1-* and *rad53-* mutant strains and *dun1Δ* cells exhibit a ~ 40%reduction in dNTP pool (Zhao et al., 2001). *sml1Δ,* on the other hand, confers a ~2 fold increase in dNTP levels (Zhao et al., 1998). Furthermore, Mec1 promotes Sml1 destruction at the onset of S phase during unchallenged proliferation (Zhao et al, 2001; Earp et al., 2015). Together, these findings led to the notion that *mec1* lethality stems from inability to remove Sml1 and the ensuing dNTP pool depletion during S phase followed by replication fork stalling and irreversible fork collapse.

mec1-4 is a hypomorphic allele that confers sensitivity to HU (hydroxyurea), MMS (methylmethane sulfonate) and heat (Cha and Kleckner, 2002). At a restrictive temperature, *mec1-4* cells exhibit permanent replication fork stalling followed by DNA double strand break formation and cell death. Surprisingly, *mec1-4* cells exhibit only a modest 17% reduction in dNTP pool (Earp et al., 2015). Findings that *mec1/rad53* hypomorphs and *dun1Δ* cells are viable and proficient in DNA replication, despite a ~40% reduction in dNTP pool, whereas *mec1-4* cells with a 17% reduction exhibit profound replication defects linked to cell death, suggest that *mec1* lethality might be independent of dNTP.

Recent studies indicate that mammalian ATM and ATR play critical roles in protein homeostasis (Cheng et al., 2018; Lee et al., 2018). Protein homoestasis is essential for life because it ensures a finely calibrated proteome necessary for cellular function and survival. Proteostasis is maintained by controlled protein synthesis, modification, trafficking, and degradation, as well as the protein quality control (PQC), which functions to minimize levels of misfolded-, damaged-, and aggregated-proteins (Hill et al., 2017; Morimoto, 2008). In human disease, the PQC is linked to aging, degenerative motor-neuron diseases (e.g. Parkinson's and Huntington's diseases) and cancer (Dai et al., 2012; Hill et al., 2017). Notably, Cheng et al (2018) found that ATM and ATR associate with neuronal synaptic vesicles and impact their trafficking. Lee et al (2018) found that an ATM allele impaired in oxidative stress-response confers sensitivity to proteotoxic stress and widespread protein aggregation. Here, we show that Mec1 is also required for survival in response to proteotoxic stresses; thus, proteostasis appears to be an evolutionarily conserved function of ATM/ATR family proteins.

RESULTS AND DISCUSSION

Unbiased screen for genetic interactors of *mec1-4* identifies genes involved in proteostasis.

To address the essential function of *MEC1* during normal proliferation, we performed synthetic genetic array (SGA) analysis of *mec1-4*. SGA is a high throughput technique for identifying genetic interactors of a gene of interest (e.g. Costanzo et al., 2010). The screen was performed using yeast deletion library and in the absence of any exogenous stress at three different temperatures, 26^{o}C, 30^{o}C, and 33^{o}C, corresponding to a permissive-, semi permissive-, and restrictive temperature of a *mec1-4* query strain, respectively (Figure S1A). In total, the screen identified hundreds of genes (Figure S1B) and to minimize inclusion of false positives, we restricted our analysis to the 200 strongest positive- and the 200 strongest negative- interactors (Figure S1B; Table S1).

The extent of overlap between *mec1-4* interactors and previously reported genetic/physical interactors of *MEC1/*Mec1 was limited (Figure 1A; Table S1). This is likely due to the fact that while our screen was performed in the absence of any exogenous stress and in an otherwise WT background, majority of previous *MEC1* studies were performed in either a *mec1Δ sml1Δ* or *mec1-kinase dead (kd) sml1Δ* background and in the presence of genotoxic- and/or replication- stress (e.g. Chen et al., 2010; Smolka et al., 2007). Nevertheless, our screen identified negative (i.e. synthetic lethal or sick) genetic interactions with a number of genes involved in well-established functions of Mec1, including DNA damage repair (e.g. *MRE11, RAD50, RAD51*), regulation of sister chromatid cohesion (e.g. *CTF4, CTF8, CTF18),* telomere maintenance (e.g. *TEL1, ELG1*), and regulation of DNA replication checkpoint (e.g. *MRC1, CMS3*) (Figure 1B; Table S1, S2). The latter provides further support for key roles of Mec1 in fundamental DNA/chromosome-

processes and mediating responses to endogenously generated genotoxic/replication stress (e.g. Desany et al., 1998; Zhao et al., 2001; Cha and Kleckner, 2002).

The *mec1-4* SGA analysis also identified both negative and positive genetic interactions with a number of genes involved in protein-homeostasis (Figure 1B; Table S3). Detailed analysis confirmed that deletion of *JJJ3, PIH1,* or *TIM18* exacerbated temperature sensitivity of *mec1-4* (Figure 1C). Jjj3 is a member of the highly conserved Hsp40/DnaJ family of molecular chaperones (Walsh et al., 2004). Pih1, *P*rotein *I*nteracting with *H*sp90, is a conserved protein involved in rRNA processing and protein folding (Zhao e al, 2005). Tim18, *T*ranslocase of the *I*nner *M*itochondrial membrane, is involved mitochondrial protein homeostasis (Kerscher et al., 2000). Deletion of *EAP1* or *KTI12,* on the other hand, rescued *mec1-4* lethality (Figure 1C). Eap1 is an eIF4E (*e*ukaryotic translation *i*nitiation *f*actor *4E*) interacting protein, involved in mRNA catabolism; and Kti12 is a protein involved in tRNA modification required for protein translation (Cosentino et al., 2000; Huang, 2005). These novel genetic interactors implicate a role of Mec1 in essential protein homeostasis.

mec1-4 lethality is linked to widespread protein aggregation.

Azetidine-2-carboxylic acid (AZC) is a proline analogue, which causes protein-misfolding and widespread protein aggregation upon incorporation into nascent polypeptides (e.g. Weids and Grant, 2014). We find that *mec1-4* cells are sensitive to AZC at 30^{o}C, a semi permissive temperature (Figure 2A red arrow). In contrast, neither a *mec1Δ sml1Δ* nor *mec1-kd sml1Δ* strain was sensitive (Figure 2A yellow arrow; data not shown). We tested two independently derived *mec1-4 sml1Δ* strains and found that the double mutants were also resistant (Figure 2A blue arrows). Together, these results suggest that Mec1 is required for resistance to AZC and that *sml1Δ* bypasses this requirement.

An *ATM* allele impaired in oxidative stress-response, *ATM-CL*, was shown to confer widespread protein aggregation in response to proteotoxic stress (Lee et al., 2018). We utilized a similar method for isolating protein aggregates to test whether *mec1-4* might also confer the phenotype (Experimental Procedures). AZC led to a notable increase in protein aggregation in a WT background (Figure 2C, D), confirming that the method in our hands also produces a semi-quantitative readout (e.g. Weids and Grant, 2014). We find that the aggregate level in *mec1-4* cells is comparable to WT following 2 hours exposure to AZC and also 2 hours after removal of AZC (Figure 2D, red arrow). In a *mec1-4 sml1Δ*strain, a notable reduction was observed following removal of AZC (Figure 2D). The latter suggests that the *sml1Δ*-dependent rescue of *mec1* sensitivity to AZC (Figure 2A, B, red arrows) might be linked to the reduction in aggregate level.

sml1Δ rescues both AZC- and temperature- sensitivity of *mec1-4,* but not its MMS or HU sensitivity (Figure 2AB; data not shown). The latter suggests that temperature sensitivity of *mec1-4* is more likely to be linked to proteotoxic stress than to genotoxic- or replication- stress. Indeed *mec1-4* cells exhibited a notably elevated level of protein aggregates following 6 hour incubation at 33^{o}C, irrespective of AZC exposure (Figure 2E, red arrow). Thus, *mec1-4* in response to heat, like ATM-CL in response to proteotoxic stress (Lee et al., 2018), leads to widespread protein aggregation. Remarkably, *sml1Δ* resulted in a dramatic reduction in the heat and *mec1-4* dependent aggregation (Figure 2E, blue arrows).

Autophagy contributes to resolution of toxic protein aggregates (e.g. Morimoto, 2008). Autophagy in yeast is shut down in a standard 2% glucose medium, but becomes activated in response to a non-fermentable carbon source such as glycerol (Okamoto et al., 2009). We confirmed that autophagy was activated in response to glycerol in both WT and

mec1-4 backgrounds (Figure S2). Results show that glycerol leads to a dramatic reduction in the heat induced protein aggregates in *mec1-4* cells (Figure 2F, red- versus blue- arrows). Furthermore, the glycerol dependent reduction is abolished in an *atg1Δ* background (Figure 2F, double blue- vs yellow-arrows); Atg1 is a serine/threonine kinase required for autophagy. We also found that glycerol rescued temperature sensitivity of *mec1-4* and that the rescue was dependent on key *ATG* genes (Figure 2G). Together, effects of heat, *sml1Δ,* and autophagy on *mec1-4* strongly suggest a causal link between protein aggregation and *mec1* lethality.

Expression of HTT103Q, an aggregation prone model peptide, is toxic to *mec1-4* cells.

Huntingtin (Htt) is an essential protein (Dragatsis et al., 1998) involved in diverse cellular processes such as vesicular trafficking, endocytosis, and autophagy. Expansion of a poly glutamine (polyQ) domain in exon 1 is linked to aberrant Htt-aggregation and onset of Huntington's Disease. A set of GFP-polypeptides containing the polyQ domain (Figure 3A) has been developed and utilized in yeast to study the molecular basis underlying Htt-aggregation. While Htt peptides that appear diffuse throughout the cell or as a single large aggregate do not affect viability, multiple smaller aggregates are cytotoxic (Figure 3B, classes I, II , and III, respectively) (e.g. Yang et al., 2016).

In our WT background, Htt25QP, Htt25Q, and Htt103QP signals were mostly diffuse Class I, whereas >50% of Htt103Q signals were Class II (Figure 3C; Table S4; data not shown). WT cells grew well at all tested temperatures (25^{o}C, 30^{o}C and 33^{o}C), irrespective of the Htt- peptide (Figure S3). In a *mec1-4* background, Htt25QP and Htt25Q signals were also mostly diffuse (data not shown). In contrast, ~ 50-65% of Htt103QP signals were Class II, while >70% of Htt103Q signals were Class III (Figure 3C-E; Table S4). We also found that

Htt103Q was toxic to *mec1-4* cells (Figure 3F, H; Figure 4B; Figure S3). Unexpectedly, these *mec1-4* phenotypes were observed not only at 30^{o}C or 33^{o}C but also 25^{o}C, revealing that the mutant cells have deficits in proteostasis even at a permissive temperature.

***mec1-4* confers resistance to cycloheximide and rescues *sml1Δ* sensitivity to the stress.**

Cycloheximide (CHX) is a bacterial toxin that inhibits the elongation step in translation. Unlike AZC, heat, and Htt103Q, which are toxic to *mec1-4* cells, CHX enhances *mec1-4* fitness (Figure 3G; red arrow). In fact, *mec1-4* confers resistance to CHX and the mutant cells grow better than WT cells, especially an elevated temperature. On the other hand, *sml1Δ* cells are acutely sensitive to CHX (Figure 3G, blue arrow). Intriguingly, *mec1-4, mec1-kd,* and *mec1Δ* alleviate the sensitivity (Figure 3G, yellow arrows). The latter suggests that Sml1 also has an active role in protein homeostasis. In further support, we find that expression of Htt103Q is toxic to *sml1Δ* cells (Figure 3H).

Key components of the Mec1 checkpoint response network are involved in mediating resistance to proteotoxic stress.

In response to genotoxic- or replication-stress, the Mec1-Rad53-Dun1 signaling cascade promotes survival (Figure 4H, green arrow). As expected, *dun1Δ* and *rad53-K277A,* a kinase dead allele, conferred sensitivity to HU and MMS (Figure 4A; data not shown). In addition, *dun1Δ* and *rad53-K277A* cells are sensitive to AZC, CHX, and/or Htt103Q (Figure 4A-C). Chk1 is another key effector kinase of Mec1 involved in regulating anaphase onset (Cohen-Fix and Koshland, 1997; Gardner et al., 1999). *chk1Δ* did not impact survival under the tested conditions (Figure 4A-C). These observations suggest that Mec1 might rely on

specific components of its checkpoint response network to mediate resistance to proteotoxic stress.

***mec1-4* carries a single amino acid alteration, impacting its kinase activity .**

DNA sequencing analysis revealed that *mec1-4* carries a single amino acid alteration at a conserved glutamate residue in the kinase domain (E2130) (Figure 4D,E). Structural analysis shows that E2130 is located near three conserved residues, D2224, N2229, and D2243, which were shown to be mutated in previous characterized kinase-dead alleles, each required for kinase activity, but dispensable for protein stability (Paciotti et al., 2001) (Figure 4E). As expected, *mec1-D2243E sml1Δ* cells were completely impaired in HU/MMS-dependent Rad53 phosphorylation; *mec1-4* cells also exhibited a notable reduction (Figure 4G). It is likely that the complete- versus partial-loss of kinase activity accounts for the inviability of the kinase-dead versus conditional lethality of *mec1-4* mutants, respectively. Combining the latter and the finding that *mec1-4* cells are sensitive to Htt103Q at 25^{o}C (Figure 3F) suggests that *mec1-4* phenotype is likely due to diminished kinase activity rather than to heat dependent denaturation of the polypeptide.

Model: Roles of Mec1 and Sml1 in proteostasis

Taken together, the results above provide evidence that that Mec1, like mammalian ATM and ATR, plays a critical role(s) in proteostasis; in addition, they show potential involvement of the Mec1 checkpoint response network. Intriguingly, survival in response to a specific proteotoxic stress appears to depend on a different set of genes: *MEC1* and *SML1* for heat (Figure 4H, red arrow), *RAD53* and *SML1* for CHX (Figure 4H, yellow arrow), and *MEC1, RAD53, DUN1,* and *SML1* for AZC (Figure 4I, blue). This suggests that Mec1

checkpoint response network might be a highly adaptable signaling module capable of responding to many different types of stresses. While the underlying molecular basis remains elusive, a likely possibility would be a stress-specific downstream target(s) of Mec1, Rad53, and/or Dun1.

Roles of Sml1 in proteostasis remains enigmatic: *sml1Δ* rescues AZC- and heat-sensitivity of *mec1-4* (Figure 2A,B), which suggested that Sml1 might normally undergo degradation, analogous to what happens during the canonical checkpoint response (Figure 4H, green arrow). Unexpectedly, we found that Sml1 persisted in response to AZC or heat (Figure 4H; data not shown), reminiscent of Sml1-stabilization in response to cadmium, a proteotoxic agent (Baek et al., 2012). A speculative scenario might be that Sml1 undergoes a structural and/or functional change(s) that promotes survival (Figure 4H, Sml1*).

Furthermore, *sml1Δ* cells are acutely sensitive to CHX and *mec1-4, mec1-kd,* or *mec1Δ* rescues the sensitivity. A plausible possibility might be that Mec1 functions to down regulate protein translation in response to proteotoxic stress (i.e. analogous to down regulating DNA replication in response to genotoxic/replication stress), whereas Sml1 normally functions to promote translation. According to this scenario, *sml1Δ* cells would be compromised for translation and therefore sensitive to CHX. *mec1* would be impaired in down regulating translation and thus able to alleviate CHX sensitivity of *sml1Δ;* this could also account for resistance of *mec1-4* to CHX.

Could perturbation in proteostasis account for the observed dNTP pool reduction and replication fork stalling/collapse in *mec1* mutants? Several reports linking proteostasis and DNA replication provide critical insights: (i) HU is a proteotoxic radical scavenger that blocks dNTP synthesis by taking away a tyrosyl radical located in the reaction center of RNR, which initiates the catalysis (Nordlund and Reichard, 2006). (ii) HU-cytotoxicity is

dependent on its proteotoxic effects (Davies et al., 2009). (iii) HU-cytotoxicity is independent of RNR- inhibition (Davies et al., 2009). And (iv) emetine, a plant toxin widely utilized for mapping mammalian replication origins because it causes okazaki fragment-accumulation, is a translation inhibitor (Burhans et al., 1991). Combining these with evidence above suggests that perturbation in proteostasis could account for the reduced dNTP pool size, replication fork instability, and cell death in *mec1* mutants.

ATM inactivation in humans leads to A-T, a hallmark of which is neurodegeneration (Shiloh and Kastan, 2001). It has been proposed that the pathology is due to heightened sensitivity of neuronal cells to DNA damage. Notably, the Htt103Q sensitivity of *mec1-4* (above) combined with recently revealed roles of ATR/ATR in neuronal vesicle trafficking (Cheng et al, 2018), suggests an alternative/additional mechanism underlying the pathology; perturbation in protein homeostasis leading to neuronal cell death.

EXPERIMENTAL PROCEDURES

Yeast strains and media

Strains utilized in current study are listed in Table S5. AZC, CHX, HU or MMS was added to YPD (1% [w/v] yeast extract, 2% (w/v) bacto peptone, 2% (w/v) glucose) at the concentration specified in each Figure. For Htt-peptide experiment, cells were incubated in uracil drop out media (ura do) supplemented with either 2% glucose or 2% galactose. For autophagy induction, cells were cultured in synthetic complete media (SC) (Baryshnikova et al., 2010) supplanted with 2% glycerol.

Analysis of insoluble protein aggregates

Cells corresponding to 20 units of OD_{600} were pelleted and resuspended in 300ul lysis buffer (50 mM potassium phosphate buffer, pH 7.0, 1 mM EDTA, 5% glycerol, 1 mM

phenylmethylsulfonyl fluoride, and 30ul of protease inhibitor cocktail [Sigma P8215]). Cells were lysed at 30°C for 30 mins after addition of 75ul of zymolase 20T (10mg/ml). Breakage of spheroplasts was achieved by sonication (Bioruptor UCD-200, Diagenode: 8x5 s, level 5). Unbroken cells and spheroplasts were removed by centrifugation at 3000 rpm, 4°C for 15 minutes. The remaining protein preparations were adjusted to equal concentration using Bradford protein assay kit (Biorad, #5000204). The membrane-associated and aggregated-proteins were isolated by centrifugation at maximum speed at 4°C for 20 minutes. The membrane-proteins were removed by washing twice with 400 µl of lysis buffer containing 10% Igepal-CA630, followed by another two rounds of washing by lysis buffer without any detergent. The remaining detergent resistant insoluble protein fractions were resuspended in SDS-PAGD sample buffer and boiled. Proteins were separated by 12% reducing SDS-PAGE and visualized by silver stain kit (Biorad, #1610449).

Htt-GFP morphology

Following an overnight incubation in 2% glucose ura do media (25^{o}C), cultures were diluted and further incubation until they reached mid log phase. Cells were washed and divided into two and resuspended in either 2% glucose or 2% galactose ura do media that had been pre- warmed to either 25^{o}C, 30 ^{o}C, 33 ^{o}C, or 37 ^{o}C. Samples samples were analyzed after 2 hours incubation at the indicated temperatures. Images were obtained using a conventional fluorescence microscope, Zeiss Axioskop 2Plus with AxioCamMR camera, and a 100x oil lens with NA 1.4 objective.

Western blot analysis

Western blot analysis was performed on TCA 20% (trichloroacetic acid) extracts prepared from culture volumes corresponding to 10 OD_{600} units. Protein extracts were precipitated and pellets were resuspended in loading buffer. After boiling, samples were

loaded on 7.5% polyacrylamide gels. Sml1 was detected with rabbit α-Sml1 antibody (Agrisera AS10 847, 1:1000). Rad53 was detected with mouse α-Rad53 antibody [EL7.E1] (ab166859, 1:1000). GFP was detected with mouse α-GFP antibody (Roche 11814460001, 1:5000). Secondary antibodies used were goat α-Mouse IgG H&L (Abcam Ab6789, 1:10000) and α-Rabbit IgG (Cell Signalling #7074, 1:5000). Secondary antibodies were detected using Western Lightning ECL Pro (PerkinElmer).

AUTHOR CONTRIBUTIONS

A.J. constructed the query strain for SGA analysis. M.C. and C.B. designed and conducted the SGA analysis. E.W. performed the DNA sequencing analysis of *mec1-4* and constructed the molecular model. I.C., K.Z. and R.C designed and conducted the experiments. R.C. wrote the manuscript with inputs from I.C., K.Z., and C.B.

ACKNOWLEDGEMENT

The authors thank Thomas Nystrom, Chris Grant, and Yoshinori Ohsumi for strains and plasmid, Thomas Nystrom for insightful discussions on proteostasis and Steve Smerdon on structural impact of the *mec1-4* mutation. This work was supported by grants from North West Cancer Research to R.C., I.C., and K.D.

SUPPLEMTARY INFORMATION (SI)

SI consists of three figures and four tables:

Figure S1. Synthetic Genetic Array (SGA) analysis of *mec1-4.* Related to Figure 1 and Table S1.

Figure S2. Autophagy induction in WT and *mec1-4* cells in response to glycerol. Related to

Figure 2.

Figure S3. Impact of Htt-model peptides on WT- and *mec1-4* growth. Related to Figure 3.

Table S1. Lists of *mec1-4* genetic interactors identified in SGA screen and previously reported Mec1/*MEC1* interactors. Related to Figure 1.

Table S2. GO terms enriched among the 39 genes common to the previously reported- and SGA-sets. Related to Figure 1.

Table S3. GO terms enriched among the genes found exclusively in the SGA set. Related to Figure 2.

Table S4. Htt peptide morphology in *MEC1* and *mec1-4*. Related to Figure 3.

Table S5. List of strains utilized.

REFERENCES

Baek, I.J., Kang, H.J., Chang, M., Choi, I.D., Kang, C.M., and Yun, C.W. (2012). Cadmium inhibits the protein degradation of Sml1 by inhibiting the phosphorylation of Sml1 in Saccharomyces cerevisiae. Biochem. Biophys. Res. Commun. *424*, 385–390.

Burhans, W.C., Vassilev, L.T., Wu, J., Sogo, J.M., Nallaseth, F.S., and Depamphilis, M.L. (1991). Emetine allows identification of origins of mammalian DNA replication by imbalanced DNA synthesis, not through conservative nucleosome segregation. *10*, 4351–4360.

Carballo, J.A., Johnson, A.L., Sedgwick, S.G., and Cha, R.S. (2008). Phosphorylation of the Axial Element Protein Hop1 by Mec1/Tel1 Ensures Meiotic Interhomolog Recombination. Cell *132*, 758–770.

Cha, R.S., and Kleckner, N. (2002). ATR homolog Mec1 promotes fork progression, thus averting breaks in replication slow zones. Science (80-.). *297*.

Chabes, A., Domkin, V., and Thelander, L. (1999). Yeast Sml1, a protein inhibitor of ribonucleotide reductase. J. Biol. Chem. *274*, 36679–36683.

Chen, S.H., Albuquerque, C.P., Liang, J., Suhandynata, R.T., and Zhou, H. (2010). A proteome-wide analysis of kinase-substrate network in the DNA damage response. J. Biol. Chem. *285*, 12803–12812.

Cohen-Fix, O., and Koshland, D. (1997). The anaphase inhibitor of Saccharomyces cerevisiae Pds1p is a target of the DNA damage checkpoint pathway. Proc. Natl. Acad. Sci. U. S. A. *94*, 14361–14366.

Cosentino, G.P., Schmelzle, T., Haghighat, A., Helliwell, S.B., Hall, M.N., and Sonenberg, N. (2000). Eap1p, a novel eukaryotic translation initiation factor 4E-associated protein in Saccharomyces cerevisiae. Mol. Cell. Biol. *20*, 4604–4613. Costanzo, M., Baryshnikova, A., Bellay, J., Kim, Y., Spear, E.D., Sevier, C.S., Ding, H., Koh, J.L.Y., Toufighi, K., Mostafavi, S., et al. (2010). The genetic landscape of a cell. Science *327*, 425–431.

Dai, C., Dai, S., and Cao, J. (2012). Proteotoxic stress of cancer: Implication of the heat-shock response in oncogenesis. J. Cell. Physiol. *227*, 2982–2987.

Davies, B.W., Kohanski, M.A., Simmons, L.A., Winkler, J.A., Collins, J.J., and Walker, G.C. (2009). Hydroxyurea Induces Hydroxyl Radical-Mediated Cell Death in Escherichia coli. Mol. Cell *36*, 845–860.

Desany, B.A., Alcasabas, A.A., Bachant, J.B., and Elledge, S.J. (1998). Recovery from DNA replicational stress is the essential function of the S-phase checkpoint pathway. Genes Dev. *12*, 2956–2970.

Dragatsis, I., Efstratiadis, A., and Zeitlin, S. (1998). Mouse mutant embryos lacking huntingtin are rescued from lethality by wild-type extraembryonic tissues. Development *125*, 1529–1539.

Earp, C., Rowbotham, S., Merenyi, G., Chabes, A., and Cha, R.S. (2015). S phase block following MEC1ATR inactivation occurs without severe dNTP depletion. Biol. Open *2*, 1739–1743.

Gardner, R., Putnam, C.W., Weinert, T., Allen, J., Zhou, Z., Siede, W., Friedberg, E., Elledge, S., Amon, A., Surana, U., et al. (1999). RAD53, DUN1 and PDS1 define two parallel G2/M checkpoint pathways in budding yeast. EMBO J. *18*, 3173–3185.

Harper, J.W., and Elledge, S.J. (2007). The DNA Damage Response: Ten Years After. Mol. Cell *28*,

739–745.

Hill, S.M., Hanzén, S., and Nyström, T. (2017). Restricted access: spatial sequestration of damaged proteins during stress and aging. EMBO Rep. *18*, 377–391.

HUANG, B. (2005). An early step in wobble uridine tRNA modification requires the Elongator complex. RNA *11*, 424–436.

Jeggo, P.A., Pearl, L.H., and Carr, A.M. (2016). DNA repair, genome stability and cancer: a historical perspective. Nat. Rev. Cancer *16*, 35–42.

Kerscher, O., Sepuri, N.B., and Jensen, R.E. (2000). Tim18p is a new component of the {Tim54p-Tim22p} translocon in the mitochondrial inner membrane. Mol. Biol. Cell *11*, 103–116.

Mallory, J.C., and Petes, T.D. (2000). Protein kinase activity of Tel1p and Mec1p, two Saccharomyces cerevisiae proteins related to the human ATM protein kinase. Proc. Natl. Acad. Sci. U. S. A. *97*, 13749–13754.

Morimoto, R.I. (2008). Proteotoxic stress and inducible chaperone networks in neurodegenerative disease and aging. Genes Dev. *22*, 1427–1438.

Nordlund, P., and Reichard, P. (2006). Ribonucleotide Reductases. Annu. Rev. Biochem. *75*, 681–706.

Okamoto, K., Kondo-Okamoto, N., and Ohsumi, Y. (2009). Mitochondria-Anchored Receptor Atg32 Mediates Degradation of Mitochondria via Selective Autophagy. Dev. Cell *17*, 87–97.

Paciotti, V., Clerici, M., Scotti, M., Lucchini, G., and Longhese, M.P. (2001). Characterization of mec1 kinase-deficient mutants and of new hypomorphic mec1 alleles impairing subsets of the DNA damage response pathway. Mol. Cell. Biol. *21*, 3913–3925.

Planta, R.J., and Mager, W.H. (1998). The list of cytoplasmic ribosomal proteins of Saccharomyces cerevisiae. Yeast *14*, 471–477.

Robinson, M.D., Grigull, J., Mohammad, N., and Hughes, T.R. (2002). FunSpec: a web-based cluster interpreter for yeast. BMC Bioinformatics *3*, 35.

Sanchez, Y., Bachant, J., Wang, H., Hu, F., Liu, D., Tetzlaff, M., and Elledge, S.J. (1999). Control of the

DNA Damage Checkpoint by Chk1 and Rad53 Protein Kinases Through Distinct Mechanisms. Science (80-.). *286*, 1166–1171.

Shiloh, Y., and Kastan, M.B. (2001). ATM: Genome stability, neuronal development, and cancer cross paths. Adv. Cancer Res. *83*, 209–254.

Smolka, M.B., Albuquerque, C.P., Chen, S., and Zhou, H. (2007). Proteome-wide identification of in vivo targets of DNA damage checkpoint kinases. Proc. Natl. Acad. Sci. U. S. A. *104*, 10364–10369.

Walsh, P., Bursać, D., Law, Y.C., Cyr, D., and Lithgow, T. (2004). The J-protein family: modulating protein assembly, disassembly and translocation. EMBO Rep. *5*, 567 LP-571.

Wang, X., Ran, T., Zhang, X., Xin, J., Zhang, Z., Wu, T., Wang, W., and Cai, G. (2017). 3.9 Å structure of the yeast Mec1-Ddc2 complex, a homolog of human ATR-ATRIP. Science (80-.). *358*, 1206–1209.

Weinert, T.A., Kiser, G.L., and Hartwell, L.H. (1994). Mitotic checkpoint genes in budding yeast and the dependence of mitosis on DNA replication and repair. Genes Dev. *8*, 652–665.

Yang, J., Hao, X., Cao, X., Liu, B., and Nyström, T. (2016). Spatial sequestration and detoxification of huntingtin by the ribosome quality control complex. Elife *5*.

Yi, C., Tong, J., Lu, P., Wang, Y., Zhang, J., Sun, C., Yuan, K., Xue, R., Zou, B., Li, N., et al. (2017). Formation of a Snf1-Mec1-Atg1 Module on Mitochondria Governs Energy Deprivation-Induced Autophagy by Regulating Mitochondrial Respiration. Dev. Cell *41*, 59–71.e4.

Zhao, X., and Rothstein, R. (2002). The Dun1 checkpoint kinase phosphorylates and regulates the ribonucleotide reductase inhibitor Sml1. Proc. Natl. Acad. Sci. U. S. A. *99*, 3746–3751.

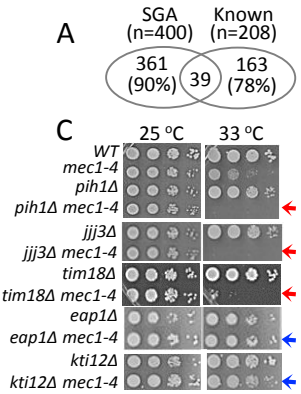

B

SGA ∩ Known (n=39)

GO Term	p-value
Response to DNA damage stimulus	1.0 e-14
DNA repair	1.0 e-14
Mitotic sister chromatid cohesion	4.6 e-11
DNA Replication	8.8 e-9
Telomere maintenance	9.9 e-7
DNA replication checkpoint	5.0 e-4

Exclusively in SGA (n=361)

GO Term	p-value
Structural constituent of ribosome	1.2 e-7
Translation	4.4 e-5
Polysome	4.0 e-4
rRNA export from nucleus	7.4 e-4
Proteosome assembly	9.6 e-3

Figure 1. Synthetic Genetic Array (SGA) analysis of *mec1-4* identifies novel genetic interactors involved in proteostasis.

A. Limited overlap between SGA hits ("SGA") (Figure S1; Table S1) and 208 previously reported genetic/physical interactors of Mec1/*MEC1* ("Known") (Table S1). %: The percentage of genes unique to either set.

B. Upper panel: GO (Gene Ontology) terms enriched in the 39 genes common to both sets. Lower panel: GO terms enriched in the 361 genes found exclusively in the SGA (Tables S2, S3). The analysis was performed using an online tool, FunSpec (Robinson et al., 2002).

C. Indicated strains were spotted on YPD and incubated at the indicated temperatures. Blue or red: synthetic positive- or negative- interaction with *mec1-4*, respectively.

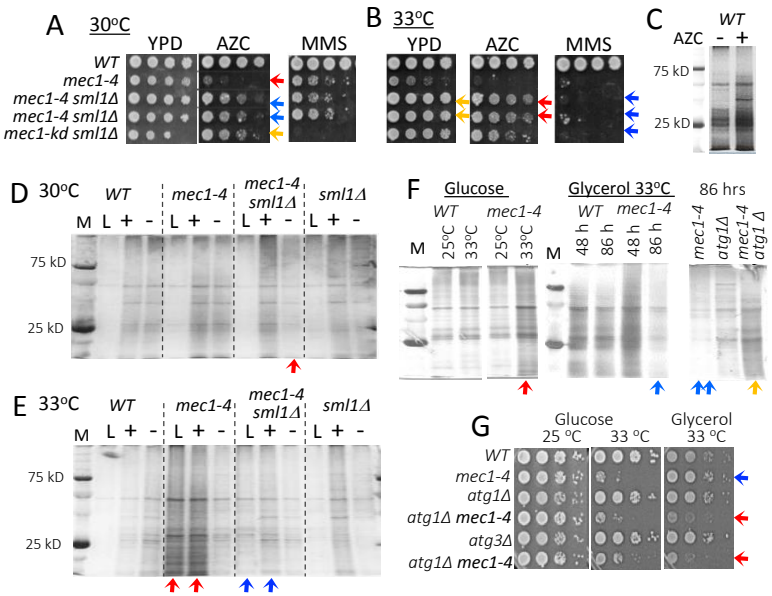

Figure 2. Causal link between widespread protein aggregation and *mec1-4* lethality.

A. Indicated strains were spotted on YPD, AZC (0.5mg/ml) or MMS (0.01%) and incubated at 30ºC. Red: AZC sensitivity of *mec1-4.* Blue: *sml1Δ* rescue of the sensitivity. Yellow: Resistance of *mec1Δ sml1Δ.*

B. Same as **A** except that the plates were incubated at 33ºC. Yellow and red versus blue: *sml1Δ* rescues *mec1-4* sensitivity to heat and AZC, but not MMS, respectively.

C. Insoluble protein aggregates in WT cells at 30oC in the absence (-) or presence (+) ofAZC (0.5mg/ml; 2 hour exposure) were isolated and analyzed as described (Experimental Procedures).

D. Indicated strains were grown overnight at 25ºC. Cells were diluted and subjected to further incubation at 30oC to mid-log phase (L). +: 2 hours AZC-exposure. -: 2 hours following AZC removal. Protein aggregates were isolated and analyzed as described (Experimental Procedures). Red: impact of *sml1Δ* on AZC and *mec1-4*-dependent aggregation following AZC-removal.

E. Same as in **D** except that the cultures were incubated at 33ºC following the 25ºC overnight incubation. Red: *mec1-4* and heat dependent protein aggregation irrespective of AZC exposure. Blue: Impact of *sml1Δ* on the aggregation.

F. "Glucose": Protein aggregates were isolated following an overnight incubation in 2% glucose medium at the indicated temperatures. "Glycerol 33ºC": Protein aggregates were isolated at the indicated time points after a glucose-to-glycerol medium switch. Red: heat induced aggregation in *mec1-4.* Blue: glycerol dependent reduction in aggregation. Yellow: glycerol dependent reduction is abolished by *atg1Δ*.

G. Glycerol-dependent rescue of *mec1-4* lethality (blue) is dependent on autophagy genes (red).

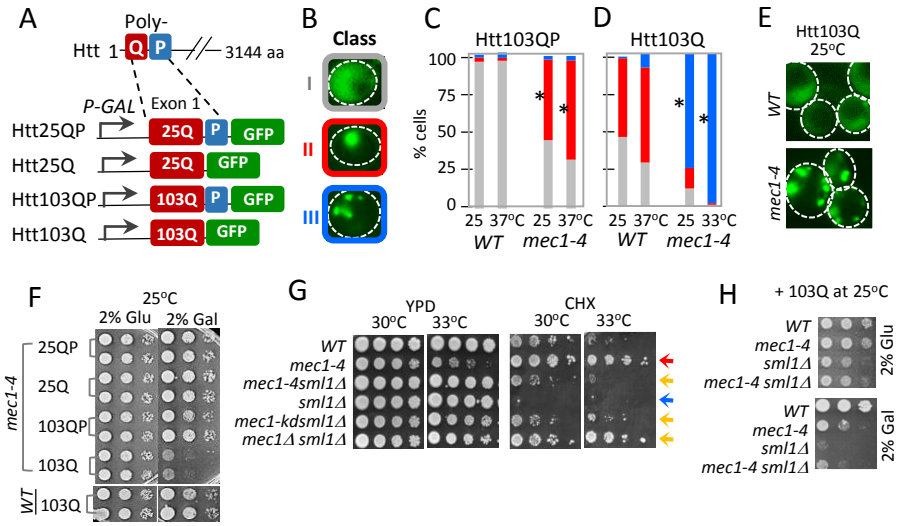

Figure 3. Htt103Q expression is toxic to *mec1-4* and *sml1Δ* cells.

A. Schematic representation of Huntingtin (Htt) plasmids utilized in current study. "Q": Poly glutamine (Q) domain; 25 and 103 indicates the number of Qs in each peptide. "P": Poly proline domain, implicated in Htt aggregation.

B. Representative images of Htt-GFP morphology. Class I: diffuse throughout the cell. Class II: a single large aggregate. Class III: multiple aggregates.

C, D. Htt103QP (**C**) and Htt103Q (**D**) morphology in *WT* and *mec1-4* cells following 2 hour incubation in galactose medium at the indicated temperatures. Grey, red, and blue: % of cells exhibiting Class I, II, or III morphology described in panel **B**, respectively. Asterisks: statistically significant increase over WT ($p < 0.005$) (Table S4).

E. Representative Htt103Q morphology in WT and *mec1-4* following 2 hour incubation in galactose medium at 25°C.

F. *mec1-4* and *WT* strains transformed with the indicated Htt-GFP plasmids were spotted onto a glucose or galactose plate and incubated at 25°C. Two independent transformants were analyzed for each Htt peptide.

G. Opposite effects of CHX on *mec1-4* and *sml1Δ.* Red: *mec1-4* confers resistance to CHX. Blue: *sml1Δ* confers sensitivity to CHX. Yellow: *mec1-4, mec1-kd*, and *mec1Δ* rescue CHX sensitivity of *sml1Δ*.

H. Htt103Q is toxic to *mec1-4, sml1Δ,* and *mec1-4 sml1Δ* at 25°C.

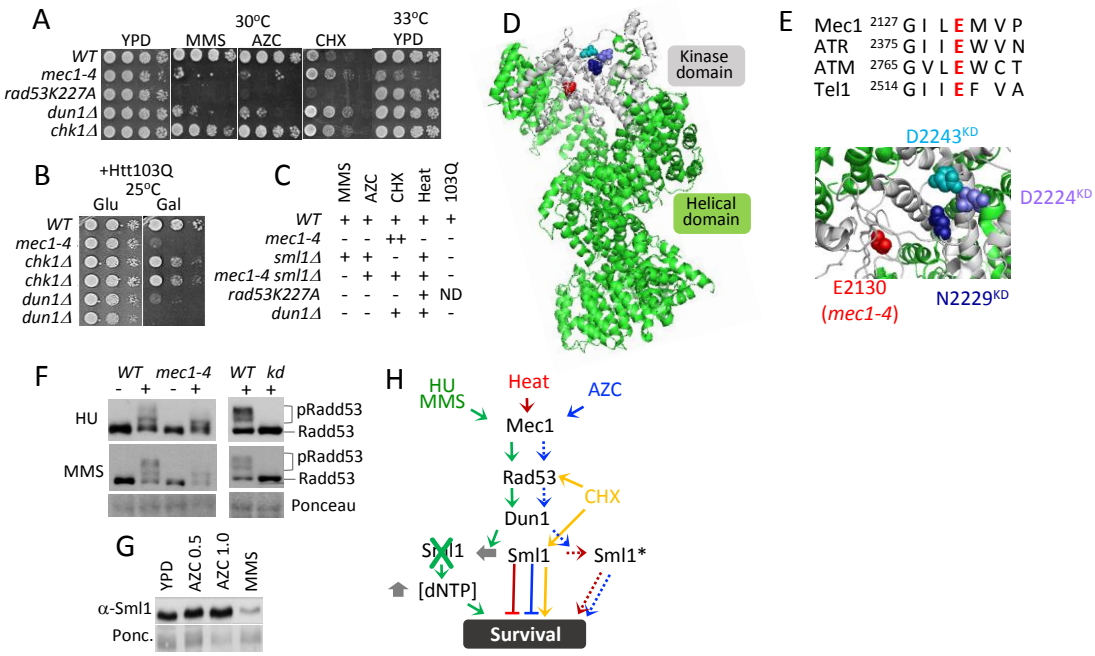

Figure 4. Mec1-checkpoint response network promotes survival in response to genotoxic, replication, and proteotoxic stress.

A. Indicated strains were spotted on YPD, MMS (0.01%), AZC (0.5 mg/ml), or CHX (0/5 ug/ml) and incubated at 30°C or 33°C.

B. Indicated strains expressing Htt103Q plasmids were spotted onto a glucose orgalactose plate and incubated at 25°C. Two independent transformants of *dun1Δ* and *chk1Δ* were analyzed.

C. Summary of spot test-results in Figures 2A, 2B, 3F, 4A, and 4B. +: WT level growth. -: reduced growth. ++: enhanced growth. ND: Not determined.

D. *mec1-4* carries a single amino acid alteration at E2130 (red) in the C-terminal kinase domain (grey). The image is generated in PyMol program based on a published Mec1 structure (Wang et al., 2017).

E. E2130 is a conserved residue and located near three residues previously shown to be required for kinase activity but dispensable for protein stability (Pacciotti, 2001).

F. Rad53 Western blot analysis (Experimental Procedures) was performed on indicated strains. -: log phase culture at 25°C. +: 2 hour incubation in 10 mM HU or 0.05% MMS at 25°C. kd: *mec1-D2243E sml1Δ.*

G. Sml1 Western blot analysis (Experimental Procedures) was performed on WT cells in log phase culture (YPD), following 2 hour exposure to either 0.5 or 1 mg/ml AZC or 0.05% MMS. All incubations were at 30°C.

H. Model: Mec1 signaling network mediates resistance to genotoxic, replication, and proteotoxic stress. Red: Survival in response to heat is dependent on Mec1 and Sml1. Blue: Survival in response to AZC requires Mec1, Rad53, Dun1, and Sml1. Yellow: Survival in CHX requires Rad53 and Sml1. Sml1*: Putative functionally and/or structurally distinct Sml1 species required for survival. Solid lines: links inferred based on findings above. Broken lines: putative links based on their roles during genotoxic/replication stress response. Green: canonical checkpoint response.

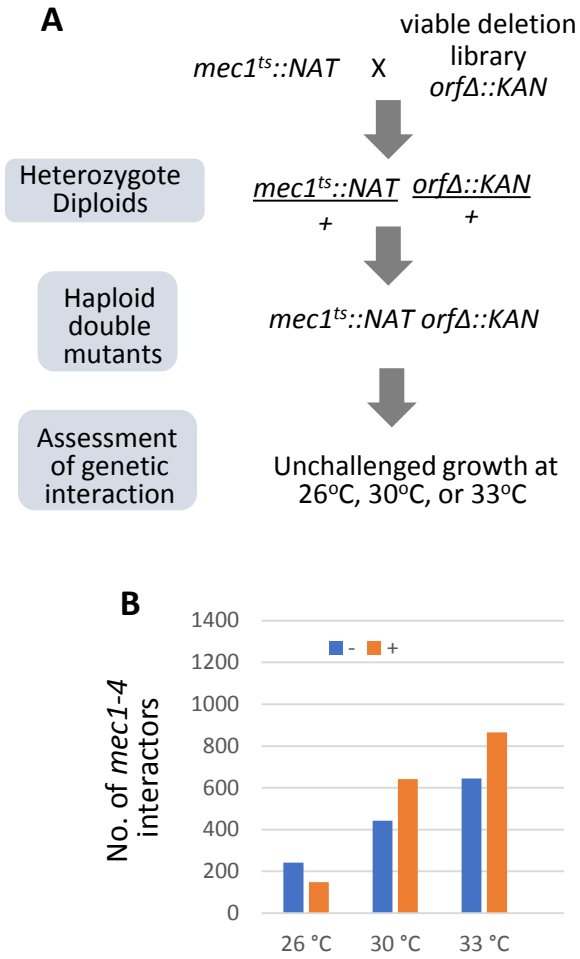

Figure S1. Synthetic Genetic Array (SGA) analysis of *mec1-4*.

A. SGA analysis of *mec1-4* was performed as described (Baryshnikova et al., 2010). Briefly, a *mec1-4::NatMX* query strain was constructed and crossed with a viable deletion library marked with *KanMX.* The resulting diploids were sporulated and selected for *MATa* double mutant haploids carrying both *mec1-4::NatMX* and a deletion mutation. Fitness of each double mutant was compared to both a *mec1-4* or the corresponding single deletion mutant on 2% glucose synthetic complete medium agar plates at 26°C, 30°C, and 33°C and positive- or negative-interaction was assessed as described (Baryshnikova et al., 2010).

B. Number of *mec1-4* genetic interactors identified at the indicated temperature. Blue and red bars represent negative- and positive-interactors, respectively. To minimise inclusion of false positives, we took advantage of the quantitative nature of the SGA analysis, and limited our analysis to the 200 strongest positive- and the 200 strongest positive- interactors.

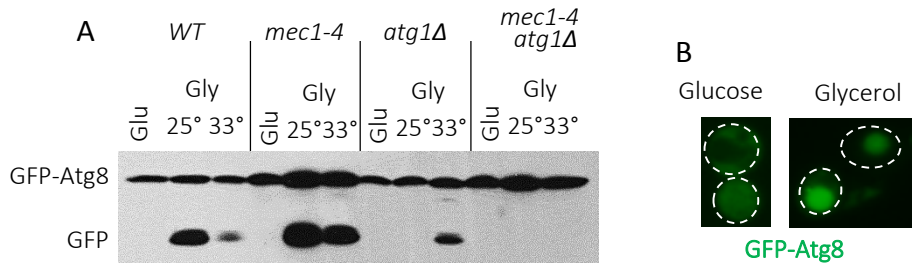

Figure S2. Glycerol dependent autophagy activation.

A. To confirm autophagy activation, we monitored the autophagy-dependent release of GFP from GFP-Atg8, a well-established read out for autophagy (e.g. Okamoto et al., 2009). Indicated strains were transformed with a plasmid carrying GFP-Atg8. Cells were grown in 2% glucose medium at 25ºC for overnight ("Glu"). Cells were washed and resuspended in 2% glycerol medium and incubated at the indicated temperatures ("Gly"). Samples were collected after 48 hours and Western blot analysis was performed using α-GFP antibody (Experimental Procedures). Appearance of GFP fragment indicates autophagy activation.

B. Glycerol-dependent autophagy is further confirmed by vacuole-localization of GFP-Atg8 in a *WT* strain 48 hours after a glucose-to-glycerol medium switch. Cells were incubated at 25ºC.

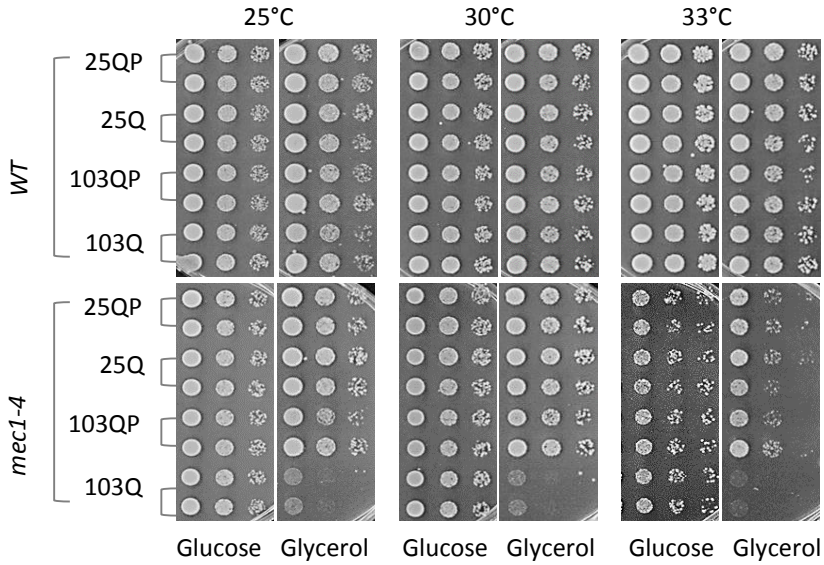

Figure S3. Impact of Htt model peptides on *WT* and *mec1-4* growth

mec1-4 and *WT* strains transformed with the indicated Htt-GFP plasmids were spotted onto a glucose or galactose plate and incubated at the indicated temperatures. Two independent transformants were analyzed for each Htt peptide.